

Article

An Optimal Sizing of Stand-Alone Hybrid PV-Fuel Cell-Battery to Desalinate Seawater at Saudi NEOM City

Hegazy Rezk ^{1,2,*} , Mohammed Alghassab ³ and Hamdy A. Ziedan ^{4,*} 

¹ College of Engineering at Wadi Addawaser, Prince Sattam Bin Abdulaziz University, Al-Kharj 11911, Saudi Arabia

² Electrical Engineering Department, Faculty of Engineering, Minia University, Minia 61517, Egypt

³ Electrical Engineering Department, College of Engineering, Shaqra University, Riyadh 11911, Saudi Arabia; malghassab@su.edu.sa

⁴ Faculty of Engineering, Assiut University, Assiut 71518, Egypt

* Correspondence: hr.hussien@psau.edu.sa (H.R.); ziedan@aun.edu.eg (H.A.Z.)

Received: 24 February 2020; Accepted: 18 March 2020; Published: 25 March 2020



Abstract: NEOM City in Saudi Arabia is planned to be the first environmentally friendly city in the world that is powered by renewable energy sources minimizing CO₂ emissions to reduce the effect of global warming according to Saudi Arabia's Vision 2030. In recent years, Saudi Arabia has had a problem with water scarcity. The main factors affecting water security are unequal water distribution, wrong use of water resources and using bad or less efficient irrigation techniques. This paper is aimed to provide a detailed feasibility and techno-economic evaluation of using several scenarios of a stand-alone hybrid renewable energy system to satisfy the electrical energy needs for an environmentally friendly seawater desalination plant which feeds 150 m⁻³ day⁻¹ of freshwater to 1000 people in NEOM City, Saudi Arabia. The first scenario is based on hybrid solar photovoltaic PV, fuel cells (FC) with a hydrogen storage system and batteries system (BS), while the second and third scenarios are based on hybrid PV/BS and PV/FC with a hydrogen storage system, respectively. HOMER[®] software was used to obtain the optimal configuration based on techno-economic analysis of each component of the hybrid renewable energy systems and an economic and environmental point of view based on the values of net present cost (NPC) and cost of energy (COE). Based on the obtained results, the best configuration is PV/FC/BS. The optimal size and related costs for the optimal size are 235 kW PV array, 30 kW FC, 144 batteries, 30 kW converter, 130 kW electrolyzer, and 25 kg hydrogen tank is considered the best option for powering a 150 m³ reverse osmosis (RO) desalination plant. The values of net present cost (NPC) and the cost of energy (COE) are \$438,657 and \$0.117/kWh, respectively. From the authors' point view, the proposed system is one among the foremost environmentally friendly systems to provide electric energy to the seawater desalination plant, especially when connecting to the utility grid, because it is ready to reduce a large amount of greenhouse gas emissions due to using oil/nature gas in utility generation stations to reduce the effect of global warming.

Keywords: Environmentally-friendly; seawater desalination plant; hybrid PV/FC/BS; hydrogen storage system; Saudi NEOM City

1. Introduction

Saudi Arabia is one of the biggest producers and net exporter of oil in the world, with more than 12% of total oil production in the world in 2018 [1] as shown in Figure 1. According to Saudi Arabia's

Vision 2030 [2], the Saudi Government is working to reduce use of fossil fuels and increase use of renewable energy.

In recent years, Saudi Arabia has had a problem with water scarcity [3]. Saudi Arabia, for supporting its rapidly growing population and development, is heavily dependent on underground water and rain which are not sufficient. Therefore, there is a shift toward using seawater desalination plants depending on renewable energy systems.

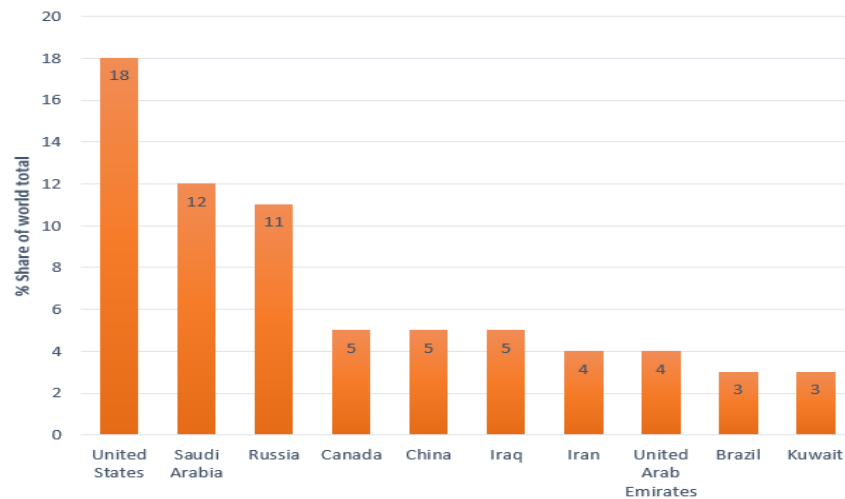


Figure 1. The largest oil producers' countries and share of total world oil production in 2018.

NEOM City is planned to be a cross-border city that shares with Egypt and Jordan borders. The site under study is close to the Red Sea in Tabuk Province of north-western Saudi Arabia with a total area of 26,500 km² and 460 km along the coast of the Red Sea (Figure 2). The Saudi government is planning to make NEOM City the first environmentally friendly city powered by renewable energy sources to minimize CO₂ emissions to reduce the effect of global warming [4,5].



Figure 2. Location of the case study of NEOM City, Saudi Arabia (www.google.com/maps).

Seawater desalination is the process that converts seawater to freshwater by removing salt particles from seawater. Different desalination processes are used in industrial and commercial applications. With improvements in technology techniques, desalination processes are becoming cost-competitive and more efficient rather than other methods of producing freshwater to overcome our growing needs [6]. However, the total cost of seawater desalination is still high with using conventional methods of energy sources. Therefore, the new trend of Saudi's governments is using renewable energy systems, which will decrease the cost of energy compared with grid extension and diesel generation systems. In addition to the cost of treatment, the environmental effects of using fossil fuel is high in the long term; CO₂ emissions have an effect on global warming.

Using renewable energy will solve one of the most pressing environmental issues and reduce the effect of global warming [6,7]. Using renewable energy systems for supplying the desalination systems with required energy has increased worldwide; more than 130 desalination plants opened in the last few years [8,9]. The salinity of the Red Sea's water is high with values of about 40,000 mg/L. Therefore, the suitable kind of desalination system for the case study is reverse osmosis (RO) [10,11].

The main sources of renewable energy that are used in desalination systems are solar PV, wind, fuel cell, geothermal, wave and tidal energies, while hydropower and biomass energies are used in minor cases. Using solar PV energy is the most preferred renewable energy technique in desalination technology based on its ability to produce heat and electric energies which are required by all desalination processes. Due to minimum operating and maintenance costs, solar PV cells can be used to secure electric energy in remote areas [12]. Solar PV energy systems are usually hybrid with other systems; batteries, diesel generators, and/or fuel cells with hydrogen tanks [13]. Due to the nature of solar energy which depends on weather conditions, cloudy or not, day and night, applications are limited by limited time periods that depend on solar energy availability [14–16].

Batteries systems (BS) are conventional storage devices used to store excessive energy in a renewable energy system. It cannot meet the storage requirements due to the global progress in renewable energy, mostly where utility connection is not available. BS plays an important role in the high energy-density and lifetime of hybrid renewable energy systems. Lead-acid batteries have disadvantages i.e., short lifetime, high cost of replacement, its performance affected by low/high air temperature and environmental concerns with used batteries [13]. Additionally, diesel generator systems have some limitations i.e., high operating and maintenance costs, high noise, pollution, cost of fuel, and transportation [14].

Electrochemical devices are used to convert directly the chemical energy into electrical energy, known as fuel cells (FC). The advantages of using FC can be listed as working with high efficiency, silent devices, low/no environmental impact, and small size when compared with other energy conversion devices [14–19]. Water FC/electrolyzer systems are used as high storage devices which are the best storage systems due to its low cost, high efficiency, easy integration with other hybrid systems, and environmental impact [20].

Figure 3 shows global statistics of renewable energy systems of hydropower, wind energy, solar PV systems, and bioenergy for the period from 2001 to 2019 [21]. The installed capacity of solar PV energy increased around the world more than using wind energy and bioenergy. On the other hand, dependence on using hydropower energy has decreased due to the high cost of installing dams in the last five years.

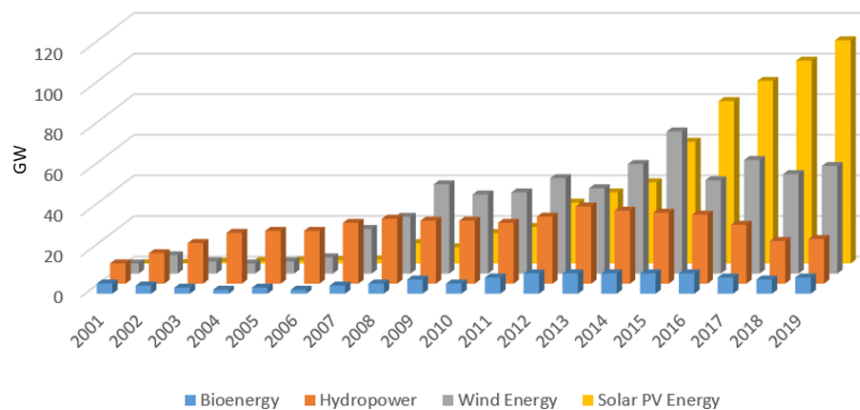


Figure 3. Global statistics of renewable energy systems for the period from 2001 to 2019.

Table 1 demonstrates a comparison of the cost results of different hybrid renewable energy systems around the world focused on Middle East countries with the proposed hybrid renewable energy system with the consideration of the size of hybrid system components, net present cost (NPC), and cost of energy (COE) which are different when compared with the proposed hybrid system.

Table 1. Summary of literature review.

Authors	Year	Location	Hybrid Configuration	Simulation Tools	NPC \$	COE \$/kWh
Shafiqur et al. [22]	2020	Pakistan	PV/WT/Battery	HOMER® MATLAB	47,398	0.309
Habib et al. [23]	2020	Pakistan	PV/WT/Battery	HOMER® MATLAB	28,620	0.311
Shafik et al. [24]	2020	Egypt	Grid/PV/WT/ Diesel G.	HOMER® NEPALN	9,670,000	0.117
Shafik et al. [24]	2020	Egypt	Grid/PV/WT	HOMER® NEPALN	9,970,000	0.177
Shafik et al. [24]	2020	Egypt	Grid/PV/Diesel G.	HOMER® NEPALN	2,770,000	0.124
Shafik et al. [24]	2020	Egypt	Grid/PV	HOMER® NEPALN	1,970,000	0.128
Shafik et al. [24]	2020	Egypt	WT/Grid/Diesel G.	HOMER® NEPALN	10,000,000	0.130
Ziedan et al. [25]	2020	Egypt	PV/WT/Battery	HOMER® MATLAB	3,461,264,640	0.202
Ziedan et al. [25]	2020	Egypt	Grid/PV/WT	HOMER® MATLAB	1,830,547,760	0.08
Al-Ghussain et al. [26]	2020	Turkey	PV/WT/Pumped Hydro Storage/ Hydrogen Fuel Cell	HOMER®	250,000	0.175
Rezk et al. [13]	2019	Egypt	PV/battery	HOMER®	109,856	0.059
Rezk et al. [14]	2019	Egypt	PV/FC	HOMER®	115,649	0.062
Habib et al. [27]	2019	Pakistan	WT/Battery	HOMER® MATLAB	14,846	0.309
Fodhil et al. [28]	2019	Algeria	PV/Diesel/Battery	PSO HOMER®	8640.1	0.37
Jahangiri et al. [29]	2019	Iran	Grid/PV/VAWTs	PSO HOMER®	84,200	0.496
Aziz et al. [30]	2019	Iraq	PV/Hydro/Diesel/Battery	HOMER®	113,201	0.054
Aziz et al. [31]	2019	Iraq	PV/Diesel G./ Battery	HOMER®	138,704	0.264
César et al. [32]	2019	Spain	PV/WT/Biomass/H2/Fuel Cell	MPC, GA MATLAB Experiment	21,161	0.123
Awan [33]	2019	Saudi Arabia	PV/WT/Diesel/Battery	HOMER®	8,130,000	0.164
Akar et al. [34]	2019	Turkey	Grid/PV	HOMER®	286,242	0.164
Jamiu et al. [35]	2019	Nigeria	PV/WT//Diesel G./Battery	HOMER®	259,354	0.218
Goudarzi et al. [36]	2019	Iran	PV/WT/Battery	HOMER®	676,345	0.274
Shaahid et al. [37]	2018	Saudi Arabia	PV/WT/Battery	HOMER®	35,449	0.226

The authors considered three scenarios for supplying the RO desalination plant in NEOM city using hybrid renewable energy systems; PV/FC/BS, PV/BS, and PV/FC. The technical and economic feasibility study was applied for the proposed hybrid system which done using HOMER[®] software to identify the optimal sizing of a hybrid system based on an environmental and economic point view based on NPC and COE. Additionally, a comparison between connection with utility and the optimal stand-alone hybrid system was undertaken. The authors can conclude from the study that a hybrid stand-alone PV/FC/BS system is the most optimal and environmentally friendly system for supplying energy to the desalination plant in NEOM city. Additionally, it is cheaper than connection to a utility extension.

2. Location of Case Study

NEOM City, the site under study is located in the north-west of Saudi Arabia very close to Egypt and Jordan borders (Figure 2), which is geographically located at the latitude of 29° north and longitude of 35° east. Figure 4 shows the solar atlas of Saudi Arabia [38] where one of the sun-belt countries is endowed with high intensity direct solar radiation. Sunshine duration throughout the year ranges from 9 to 11 h/day with few cloudy days.

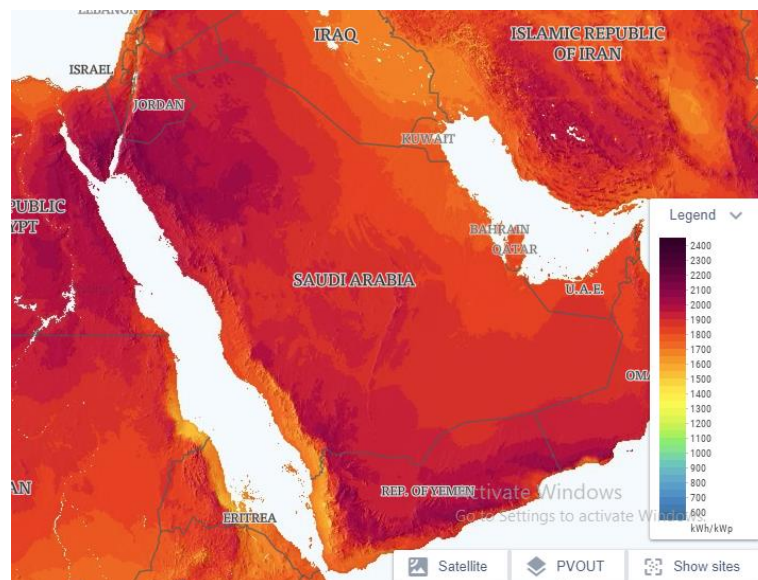


Figure 4. Solar atlas of Saudi Arabia, <https://globalsolaratlas.info/>.

Monthly mean daily solar radiation data of the site under study were obtained from NASA surface meteorology and solar energy database [39]. HOMER[®] software used this available data to calculate both the clearance index and hourly solar radiation intensity [40,41] (Figure 5). A maximum, minimum and average solar radiation intensity is 8.085 kWh m⁻² day⁻¹ in June, 3.542 kWh m⁻² day⁻¹ in December, and 5.85 kWh m⁻² day⁻¹ over the year, respectively, as shown in Figure 6. Additionally, it is clear from the available data that the site under study experiences good sunshine all year.

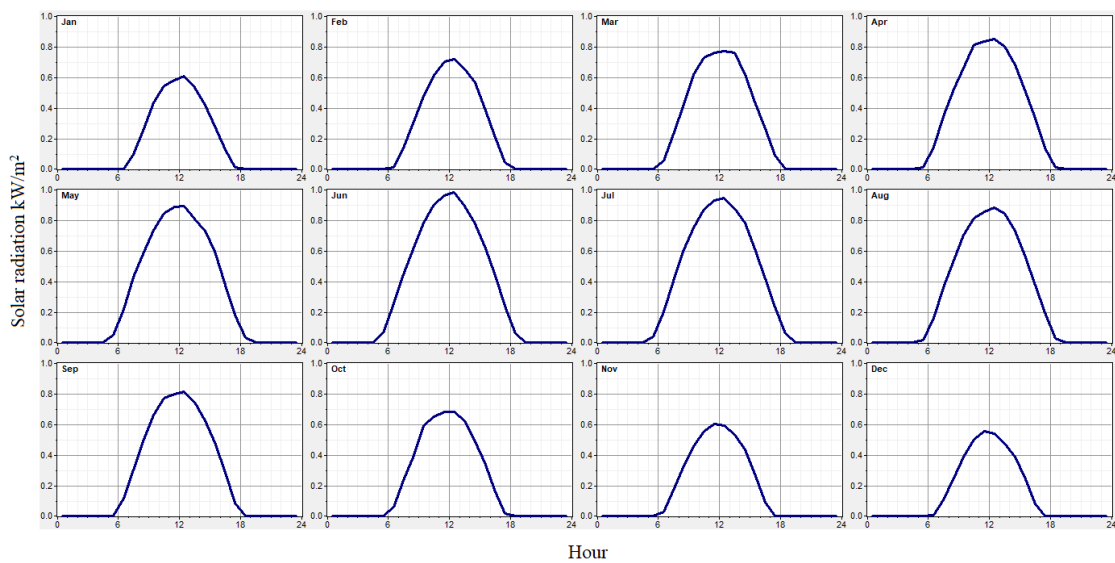


Figure 5. Variation of solar radiation intensity during the year.

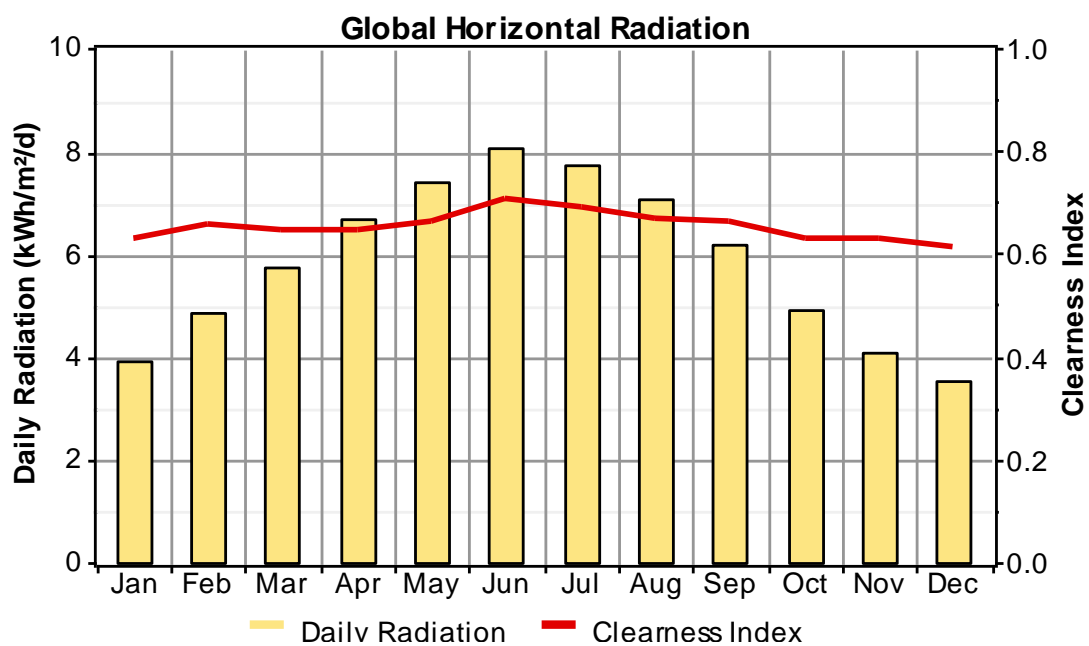


Figure 6. Average daily solar radiation and clearance index during each month.

3. Seawater Desalination Plant

The load is an electrical industrial load which is a seawater desalination plant that is supplying fresh water to 1000 people in a camp in NEOM City. Each person consumes about 150 L of freshwater in summer, per day, and 100 L in winter [42,43]. The capacity of the desalination plant is 150 and 100 m³ day⁻¹ in summer and winter, respectively. The RO unit needs the power of 522 kWh day⁻¹ with a maximum peak of 26 KW. The seasonal profile of load demand required power by the desalination plant over the year is shown in Figure 7. The RO plant will operate for 16 and 24 h, respectively, for winter and summer seasons [44,45].

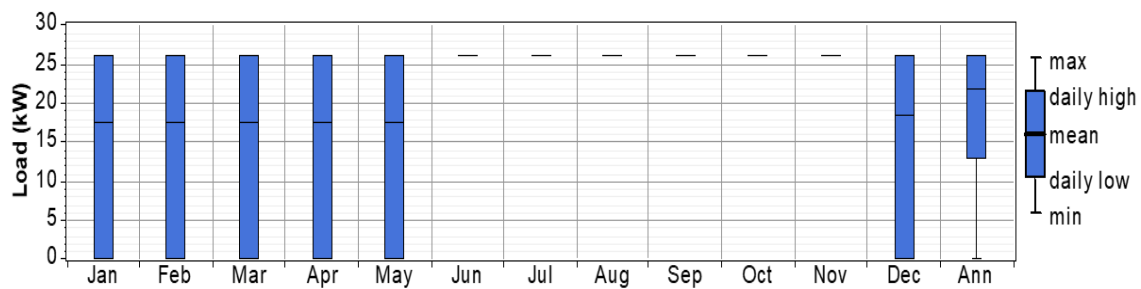


Figure 7. The seasonal profile of load demand.

Figure 8 shows a schematic diagram of the main components of the proposed seawater desalination plant [7,44]. The choice of RO unit is based on lower energy requirements and the ability to treat high saline water, $40,000 \text{ mg L}^{-1}$, from the Red Sea to achieve freshwater with high quality. A pre-filtration process with backwashing filters and cartridge filters are the standard treatment process of water [46,47].

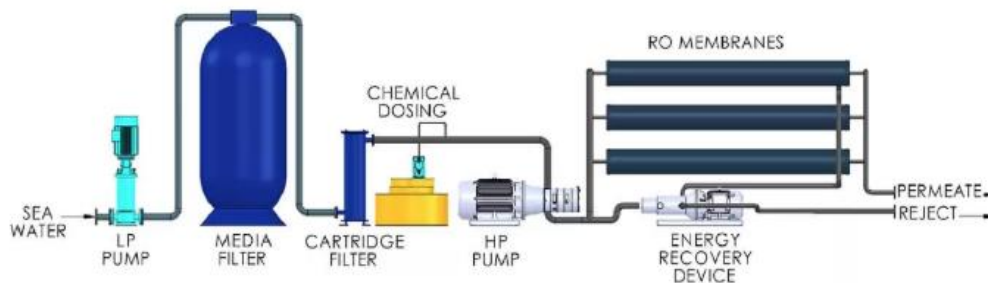


Figure 8. Schematic diagram of the main components of the proposed seawater desalination plant.

4. Description of Different Components of the System

One of the important advantages of using renewable power generators is the ability to sum two or more in one hybrid renewable system to increase the overall efficiency of the system. Figure 9 shows hybrid renewable energy systems with different scenarios for supply AC load demand, an environmentally friendly seawater desalination plant. The first scenario is based on using the PV/FC/BS system with a hydrogen storage system. The second scenario is using a PV/BS system while the third scenario is using a PV/FC system with a hydrogen storage system (Figure 9). A brief description of each component of the proposed hybrid renewable systems is summarized in the following section.

4.1. Solar PV Cells

Solar PV cells are a high power source with high economic potential. The output power from solar PV cells at any time t depends on solar radiation S and surface temperature T_c as expressed in the following equation [48]:

$$P_{PV}(t) = P_{PV_ref} * \frac{S(t)}{S_{ref}} \left[1 + \beta_{ref} (T_c(t) - T_{ref}) \right] \quad (1)$$

$$T(t) = T_a(t) + \frac{T_n - 20}{800} * S \quad (2)$$

where T_n : site under study temperature ($^{\circ}\text{C}$) at t time (h); T_n : normal operating temperature of the cell ($^{\circ}\text{C}$).

Energy from solar PV cells decreased with increasing temperature. In this study, the effect of temperature on solar PV cells was taken into account. The summary of solar PV cells data is listed in Table 2: model name: generic flat-plate PV; peak power: 1 kW; slope: 28° ; ground reflection: 27%;

operating temperature: 46°; efficiency: 14.7%; capital cost: \$1000; replacement cost: \$1000; O&M cost: \$5/year; lifetime: 25 years.

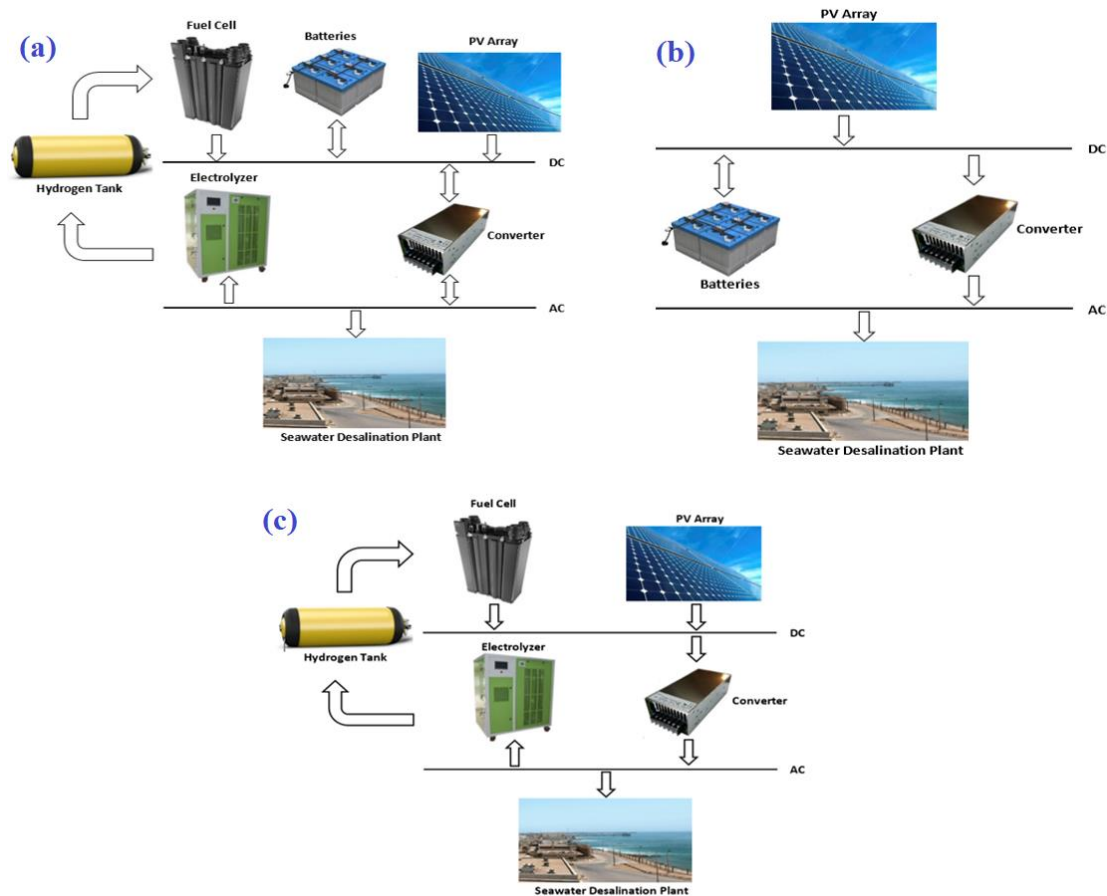


Figure 9. Schematic diagram of proposed hybrid renewable energy systems with different scenarios for supply AC load demand, an environmentally friendly seawater desalination plant; (a) first scenario: PV/FC/BS with a hydrogen storage system. (b) Second scenario: PV/BS system. (c) Third scenario: PV/FC with a hydrogen storage system.

Table 2. Summary of proposed renewable energy system components.

Component	Specification
Solar PV cells	
Model name	Generic flat-plate PV
Peak power	1 kW
Slop	28o
Ground reflection	27%
Operating temperature	46o
Efficiency	14.7%
Capital cost	\$1000
Replacement cost	\$1000
O&M cost	\$5/year
Lifetime	25 years
Fuel cell	
Model name	Proton exchange membrane
Capital cost	500 \$/kW
Replacement cost	450 \$/kW
O&M cost	0.02 \$/h
Lifetime	40,000 h
Efficiency	90%

Table 2. Cont.

Component	Specification
Batteries (BS)	
Model name	Trojan L16P
Nominal capacity	360 Ah, 2.16 kWh
capital cost	175 \$/one unit
cost of replacement	175 \$/one unit
O&M cost	5 \$/year
Converter	
Capital cost	500 \$/kW
Replacement cost	450 \$/kW
O&M cost	\$5/year
Lifetime	15 years
Efficiency	90%
Electrolyzer	
Model name	Bipolar, alkaline type
Capital cost	300 \$/kW
Replacement cost	290 \$/kW
O&M cost	5 \$/kW
Lifetime	25 years
Efficiency	85%
Hydrogen storage tank	
Capital cost	200 \$/kg
Replacement cost	150 \$/kg
O&M cost	10 \$/year.
Lifetime	25 years.

4.2. Fuel Cell

Fuel cells (FC) are electrochemical energy devices that convert the chemical energy of a fuel and hydrogen and/or oxygen into electrical energy with high efficiency approaching of 60%. FC works similar to a battery. Fuel should be continuously feeding the FC during its operation and the products of the chemical reaction should be removed continuously. Advantages of FC can be summarized as working with high efficiency, silent, and its ability to start to produce power in a short time from standby [14]. FC consists of an anode, cathode, and electrolyte. Hydrogen is fed to the anode while fresh air is fed to the cathode continuously. Output power is DC and water. The summary of FCs data is listed in Table 2 [14–18]; model name: proton exchange membrane; capital cost: \$500; replacement cost: \$450; O&M cost: \$0.02/h for a one kW; lifetime: 40,000 h.

4.3. Battery System

The battery system (BS) is used to store energy in hybrid stand-alone systems. A lead-acid battery is considered in this case study. The capacity of a battery can be calculated from the following formula [49]:

$$C_{Wh} = (E_L \times A_d) / (\eta_C \times \eta_{BS} \times D_d) \quad (3)$$

where E_L : load demand energy, kWh day⁻¹; A_d : BS autonomy, day⁻¹; D_d : discharge depth; η_{BS} and η_C are the efficiency of BS and converter, respectively. The BS data is listed in Table 2, [49–51]: type: trojan L16P, 6 V, 360 Ah; rated power: 2.16 kWh; capital cost of one unit: \$175; replacement cost: \$175; O&M cost: \$5/year; and lifetime: 1075 kWh.

4.4. Converter

Solar PV cells and FC produce DC power while the load, seawater desalination plant with RO system, needs AC power. Therefore, a DC/AC inverter is required. The converter's data is listed in Table 2: capital cost: \$500/kW; replacement cost: \$450/kW; O&M cost: \$10/year; inverter efficiency: 90%; lifetime: 10 years [50–52].

4.5. Electrolyzer

Water electrolysis technology is one of the most efficient techniques used with renewable energy systems based on hydrogen production which is non-fossil fuel. It used electricity to split water into hydrogen and oxygen [18,53]. Additionally, it is suitable for conjunction with hybrid PV cells and BS. Type of water electrolysis: bipolar, alkaline type; 10-cells in series; rated load: 250 amperes; rated voltage: 25 V; maximum power: 5 kW; purity of hydrogen gas: 99.99%; efficiency of the system: 70%; capacities of electrolyzes used in the simulation: 0–200 kW; capital cost: \$300/kW; replacement cost: \$280/kW; O&M cost: \$5/kW/year; and lifetime: 25 years as listed in Table 2 [14,51].

4.6. Hydrogen Storage Tank

To overcome the shortage of supplying energy to load demand in the night, seasonal discrepancies due to the nature of solar energy, storage energy systems should be used. The electrolyzer produces hydrogen which will be used in FC. Hydrogen storage is used to store hydrogen until it is used by FC. Hydrogen storage is better than lead-acid batteries for a long lifetime [50,51]. HOMER[®] software assumes no electricity need for supplying hydrogen to the tank and there is no leakage (Figure 9). Table 2 summarizes the data of the hydrogen storage tank [50,51]; capital cost: \$200/kg; replacement cost: \$150/kg; O&M cost: \$10/year; inverter efficiency: 90%; lifetime: 25 years.

5. Evaluation Criteria

Different scenarios were applied to obtain optimal configurations based on net present cost *NPC* and the cost of energy *COE*. *NPC* calculated based on capital costs, replacement cost, and O&M costs for the proposed lifetime and salvage value are expressed by following equation [12,14]:

$$NPC = \frac{C_{total}}{CRF(i, t)} \quad (4)$$

where *t*: the lifetime of the hybrid system; *C_{total}*: total annual cost (\$/year); *i*: annual interest rate (%); and *CRF*: capital recovery factor. The annual interest rate can be estimated as follows:

$$i = \frac{\bar{i} - f}{1 + f} \quad (5)$$

where \bar{i} : nominal interest rate; and *f*: annual inflation rate. Additionally, *CRF* can be expressed by the following equation [18,19]:

$$CRF(i, n) = \frac{i(1+n)^n}{(1+n)^n - 1} \quad (6)$$

where *n*: the lifetime of the proposed hybrid system (years) which is assumed to be 20 years. *COE* is the average cost of electrical energy unit (kWh) which can be expressed as the follows [14,22–26]:

$$COE = \frac{C_{ann_total}}{E_{total}} \quad (7)$$

where *E_{total}*: annual production energy rate (kWh/year); *C_{ann_total}*: total costs of the proposed hybrid system during the year.

6. Results and Discussion

Three different scenarios system; PV/BS, PV/FC, and PV/FC/BS were considered in the case study to determine the best option to meet the load demand. The optimal size and related costs for each considered system are shown in Table 3.

Table 3. Optimal size and related costs for each considered system.

	PV (kW)	FC (kW)	No of Batteries	Conv. (kW)	Elect. (kW)	H ₂ Tank (kg)	Initial Cost (\$)	Operating Cost (\$/yr)	NPC (\$)	COE (\$/kWh)
PV-B	155	n.a.	640	30	n.a.	n.a.	282,200	17,958	667,493	0.164
PV-FC	250	35	n.a.	30	160	90	348,500	7339	510,128	0.124
PV-FC-B	235	30	144	30	130	25	334,200	6786	438,657	0.117

Considering Table 3 that shows the optimal size and related costs for each considered system, it can be concluded that 235 kW PV array, 30 kW FC, 144 batteries, 30 kW converter, 130 kW electrolyzer, and 25 kg hydrogen tank is considered the best option for powering a 150 m³ RO desalination unit [52,54]. The values of total NPC are \$667,493, \$510,128, \$438,657, respectively, for PV/BS, PV/FC, and PV/FC/BS. The integration between BS and FC decreased the NPC by 34.28% and 13.21% compared to PV/BS and PV/FC, respectively. On the other side, the values of COE are \$0.164/kWh, \$0.124/kWh, \$0.117/kWh, respectively, for PV/BS, PV/FC, and PV/FC/BS. Under this condition using PV/FC/BS reduces the cost of energy by 28.66% and 5.6% compared to PV/BS and PV/FC, respectively. Table 4 shows the detailed related costs of different components for each considered system. Whereas, the net present cost for different system components is illustrated in Figure 10.

Table 4. Related costs of different components for each considered system.

	Capital (\$)	Replacement (\$)	O&M (\$)	Salvage (\$)	Total (\$)
PV/FC/BS					
PV array	235,000	0	25,877	0	260,877
FC	15,000	13,120	39,285	-1659	65,746
BS	25,200	43,466	15,857	-9825	74,697
Converter	15,000	12,920	0	-3899	24,021
Electrolyzer	39,000	0	14,315	0	53,315
H ₂ Tank	5000	0	0	0	5000
System	334,200	69,506	95,334	-15,383	483,657
PV/BS					
PV array	155,000	0	34,136	0	189,136
Batteries	112,000	295,608	70,474	-13,746	464,336
Converter	15,000	12,920	0	-3899	24,021
system	282,000	308,528	104,610	-17,645	677,493
PV/FC					
PV array	250,000	0	55,058	0	305,058
FC	17,500	29,949	58,535	-8554	97,430
Converter	15,000	12,920	0	-3899	24,021
Electrolyzer	48,000	0	17,619	0	65,619
H ₂ Tank	18,000	0	0	0	18,000
System	348,500	42,869	131,212	-12,453	510,128

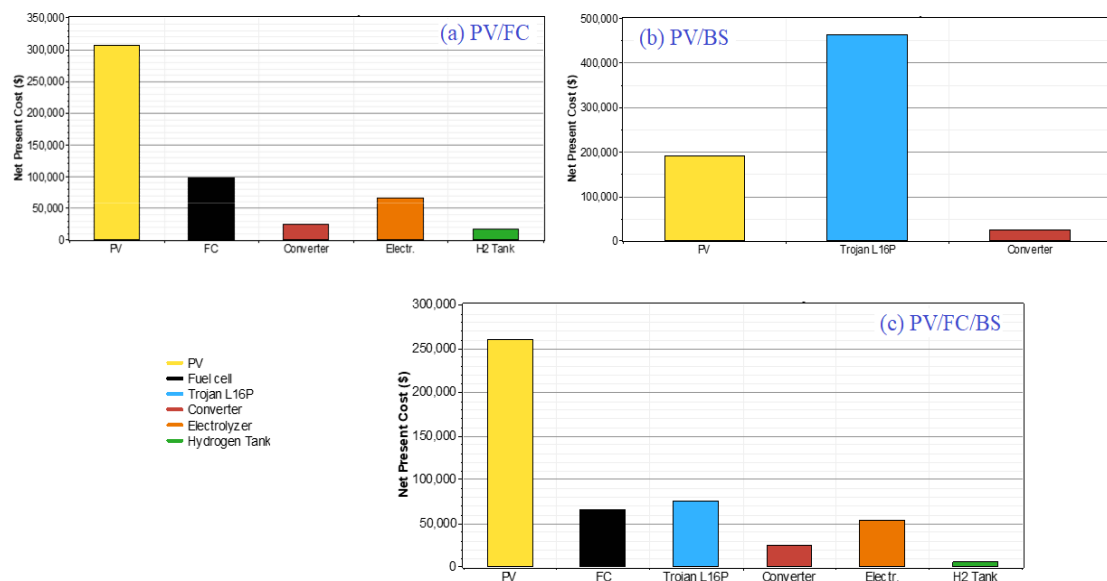


Figure 10. The net present cost for different system components.

The discounted cash flows related to every considered system is illustrated in Figure 11. As shown, the lowest initial cost is achieved by PV/BS. This due to the low cost of batteries. The initial cost values are \$282,200, \$348,500, \$334,200, respectively, for PV/BS, PV/FC, and PV/FC/BS. Due to the high replacement cost of batteries (\$295,608) as shown in Table 4, the total NPC of PV/BS increased sharply compared to PV/FC and PV/FC/BS, as illustrated in Figure 11.

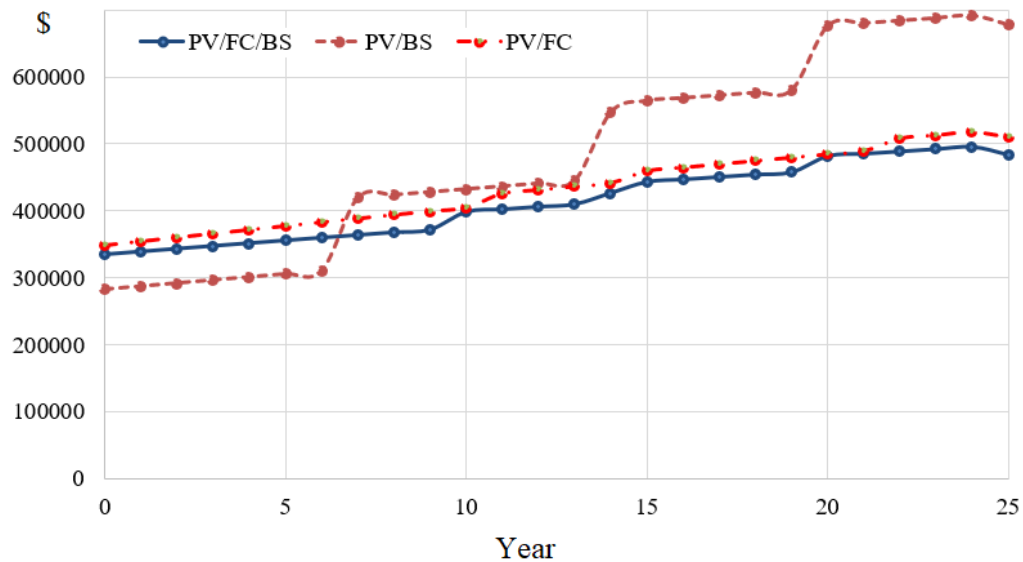


Figure 11. The discounted cash flows related to every considered system.

Under the condition of using the optimal configuration of the PV/FC/BS system, the total produced electrical energy is 542,565 kWh/yr. A total of 85% (461,155 kWh/yr) of the total energy is supplied by the PV array and the remainder (81,410 kWh/yr) comes from the fuel cell system. With this configuration, the total yearly consumption energy is 414,287 kWh. The RO unit consumed about 45% (187,134 kWh/yr) of the total consumed energy whereas as the other 55% (227,153 kWh/yr) is taken to supply the electrolyzer. The excess energy per year is approximately 105,439 (19.4%) kWh/yr. Such excess can be used for lighting and other not considered loads whereas the unmet load and capacity shortage are 3137 and 3713 kWh/yr, respectively. As illustrated in Table 5, using PV/FC/BS reduced the excess energy per year by 25.38% and 3.48%, respectively, compared with PV/BS and PV/FC. Table 6 illustrated the detailed performance of different components of the considered systems.

Table 5. Electrical energy production and consumption.

Item	Component	PV/BS	PV/FC	PV/FC/BS
Electrical production (kWh/yr)	PV	304,166 (100%)	490,590 (84%)	461,155 (85%)
	FC	n.a.	91,002 (16%)	81,410 (15%)
	Total	304,166 (100%)	581,592 (100%)	542,565 (100%)
Consumption energy (kWh/yr)	RO-unit	187,307 (100%)	187,105 (42%)	187,134 (45%)
	electrolyzer	n.a.	256,623 (58%)	227,153 (55%)
	total	187,307 (100%)	443,728 (100%)	414,287 (100%)
Excess electricity	(kwh/yr)	79,069 (26%)	117,063 (20.1%)	105,439 (19.4)
Unmet load	(kwh/yr)	3213 (1.7%)	3414 (1.8%)	3385 (1.8%)
Capacity shortage	(kwh/yr)	3822 (2%)	3978 (2.1%)	3984 (2.1%)

Table 6. The detailed performance of different components of the system.

Quantity	Units	PV/BS	PV/FC	PV/FC/BS
PV array				
Rated capacity	kW	155	250	235
Mean output	kW	35	56	53
Daily mean output	kwh	833	1344	1263
Capacity factor	%	22.4	22.4	22.4
Total production	kWh/yr	304,166	490,590	461,155
PV penetration	%	160	258	244
Hours of operation	hr/yr	4382	4382	4382
Levelized cost	\$/kWh	0.0282	0.0282	0.0257
Fuel cell				
Hours of operation	hr/yr	n.a.	3797	2973
Number of starts	Starts/yr	n.a.	573	545
Operation life	yr	n.a.	10.5	13.5
Capacity factor	%	n.a.	29.7	31
Total production	kWh/yr	n.a.	91,002	81,410
Mean electrical output	kW	n.a.	24	27.4
Min. electrical output	kW	n.a.	0.35	0.39
Min. electrical output	kW	n.a.	28.9	30
Hydrogen consumption	kg/yr	n.a.	5460	4885
Specific fuel consumption	kg/kWh	n.a.	0.06	0.06
Fuel electrical input	kWh/yr	n.a.	182,010	162,820
Mean electrical efficiency	%	n.a.	50	50
Battery storage				
Number of batteries		640	n.a.	144
Nominal capacity	kWh	1382	n.a.	311
Usable nominal capacity	kWh	968	n.a.	218
Autonomy	hr	36.7	n.a.	8.27
Lifetime throughout	kWh	688,000	n.a.	154,800
Energy in	kWh/yr	114,462	n.a.	13,557
Energy output	kWh/yr	97,495	n.a.	11,523
Storage depletion	kWh/yr	202	n.a.	0
Expected life	yr	6.51	n.a.	10
Hydrogen				
Total production	Kg/yr	n.a.	5530	4895
Levelized cost	\$/kg	n.a.	4.19	4.49
Hydrogen tank autonomy	hr	n.a.	114	31.6

The rated capacity values of PV array are 155, 250, and 235 KW, respectively, for PV/BS, PV/FC, and PV/FC/BS. Accordingly, the mean PV produced electrical energy values are 35, 56, and 53 KW for PV/BS, PV/FC, and PV/FC/BS. The detailed output production for the considered system is illustrated in Figure 12. Whereas, for the fuel cell, the mean produced energies are 24 and 27.4 KW, respectively, for PV/FC and PV/FC/BS. Approximately, June, July, and August have a maximum rate of energy production by FC. The monthly average hydrogen production for each month is shown in Figure 13.

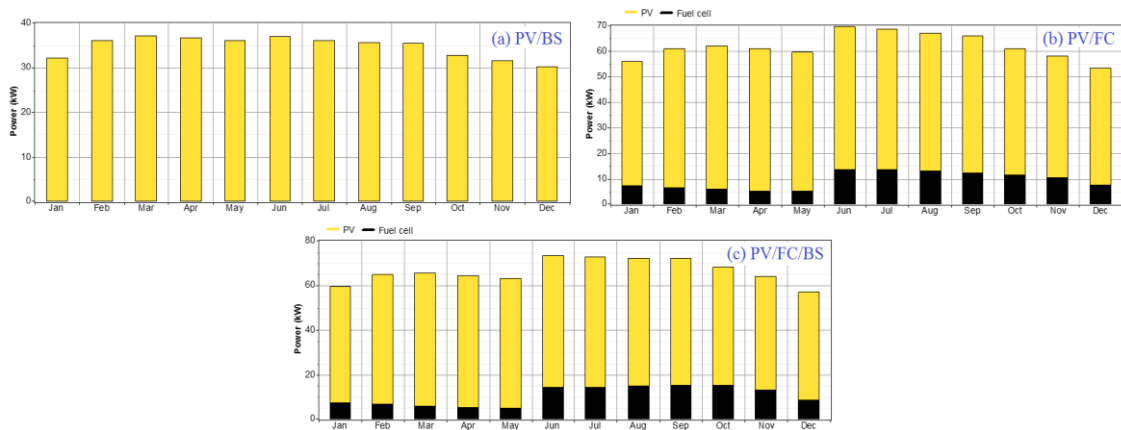


Figure 12. Average electric energy production.

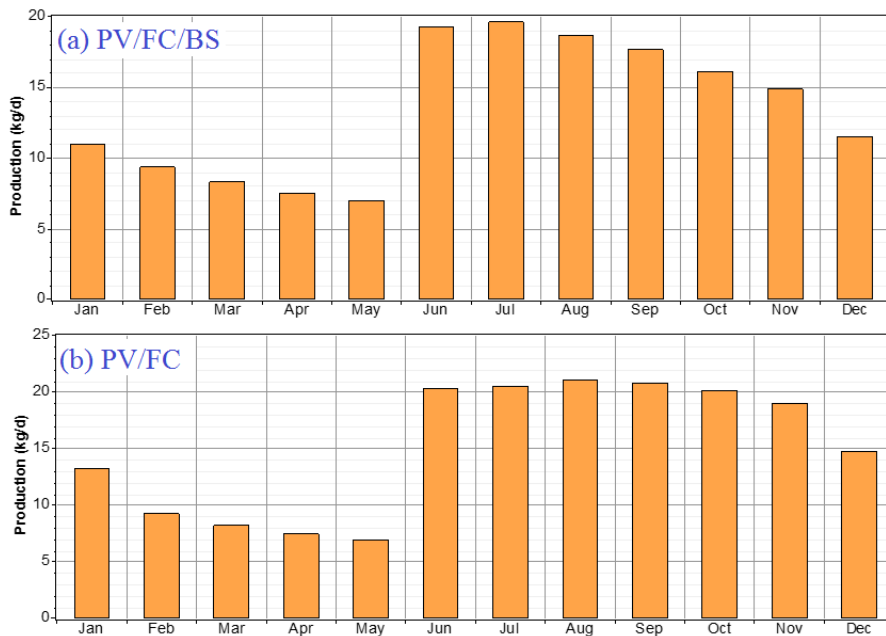


Figure 13. Monthly average hydrogen production.

The total hydrogen production per year is 5530 and 4895 kg, respectively, for PV/FC and PV/FC/BS. The hydrogen tank autonomy values are 114 h for PV/FC and 31.6 h for PV/FC/BS. The monthly statistics of the hydrogen tank is illustrated in Figure 14.

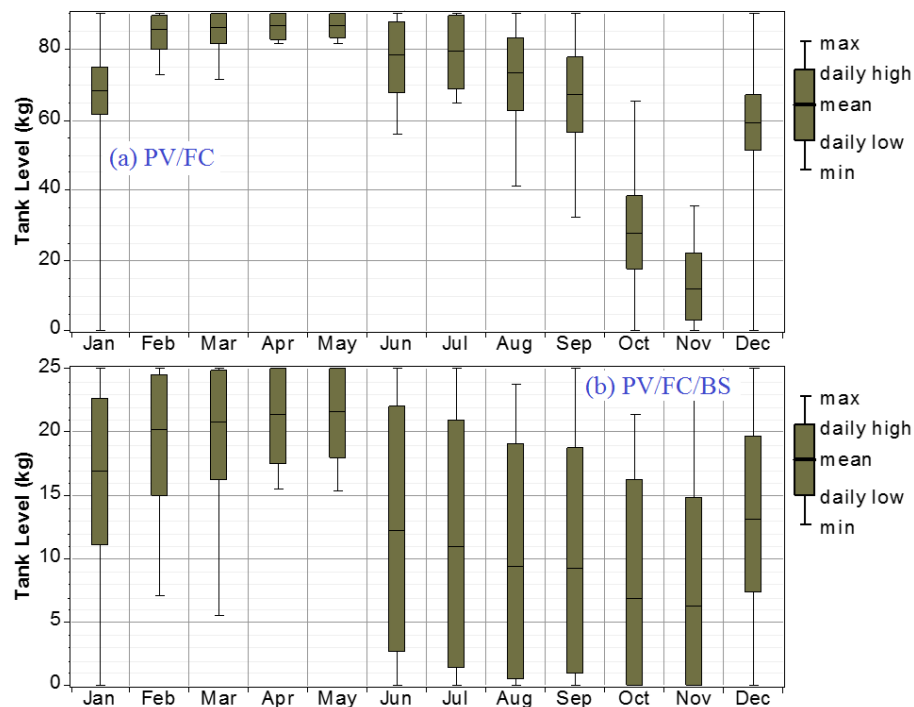


Figure 14. Monthly statistics of the hydrogen tank.

The nominal capacity values of battery are 1382 and 311 kWh, respectively, for PV/BS and PV/FC/BS. The battery autonomy values are 36.7 h for PV/BS and 8.27 h for PV/FC/BS. The expected lifetime for batteries is 6.51 and 10 years, respectively, for PV/BS and PV/FC/BS. The monthly statistics of battery state-of-charge (SOC) is illustrated in Figure 15.

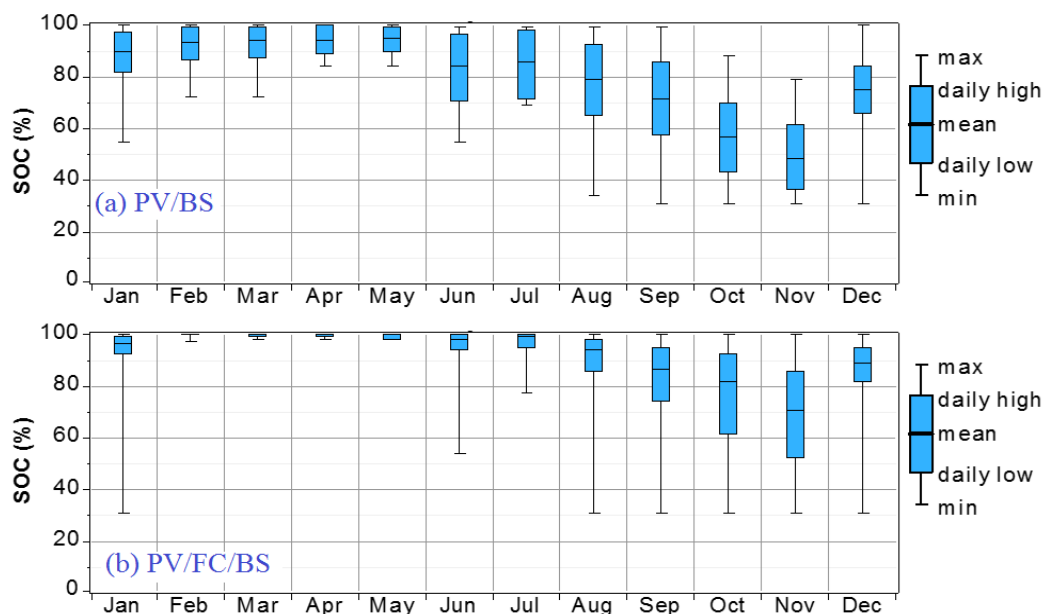


Figure 15. Monthly statistic of battery SOC.

7. Comparison with Utility Extension

A comparison between utility extension and stand-alone renewable system was undertaken to explore the optimal configuration to supply the desalination plant in NEOM city. The capital cost of the utility extinction and annual O&M costs were \$10,000/km and \$200/year/km, respectively [55].

The price of electricity from utility is \$0.06/kWh as given by the Saudi Arabia Ministry of Electricity [55]. Figure 16 shows a comparison between the total NPC of the proposed hybrid renewable systems of PV/BS, PV/FC, and PV/FC/BS, and the utility extension cost (based on the distance from the grid). Figure 16 shows that the PV/FC/BS system is better than the utility extension up to a distance of 16.1 km, while PV//FC/BS is better than the grid extension up to a distance of 26.6 km.

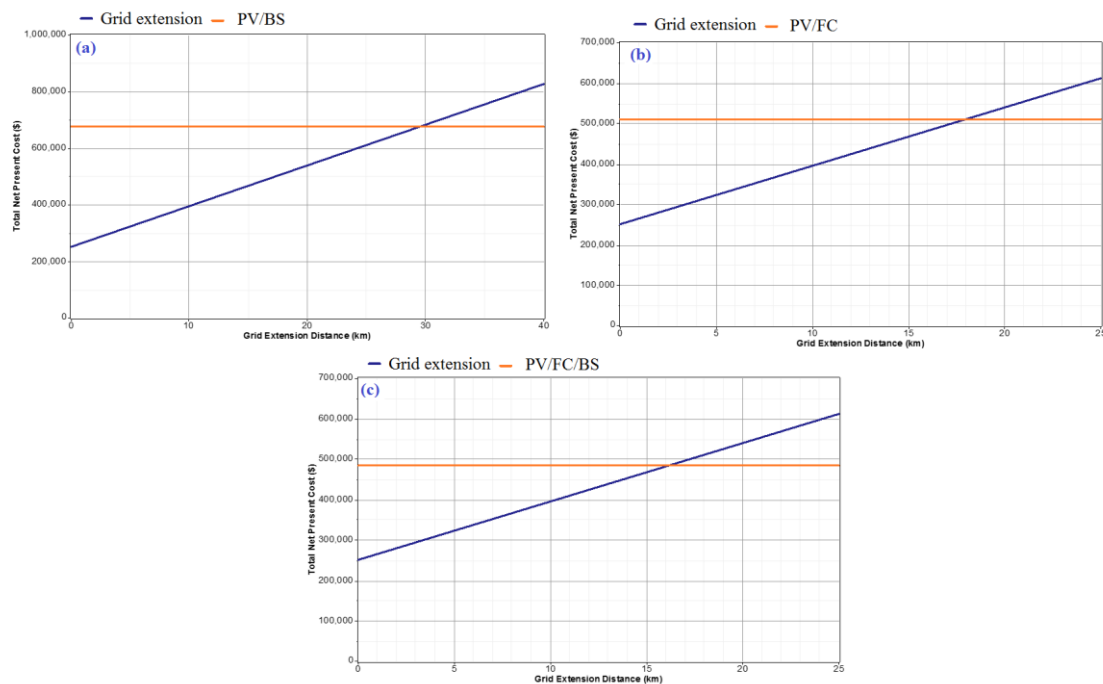


Figure 16. Breakeven grid extension distance for different systems; (a) PV/BS system. (b) PV/FC (c) PV/FC/BS.

8. Conclusions

Optimal sizing of a stand-alone hybrid PV-fuel cell-battery to desalinate seawater at Saudi NEOM city was presented in detail in this paper. The capacity of a water desalination unit is 150 m³ per day. It requires 522 kWh per day with 26 kW of maximum power. The obtained results were compared with PV/battery and PV/FC systems. The cost of energy and the total present cost were used as metrics for comparison. The optimal size of PV/FC/battery composed of 235 kW PV array, 30 kW FC, 144 batteries, 30 kW converter, 130 kW electrolyzer, and 25 kg hydrogen tank. The values of total NPC are \$667,493, \$510,128, and \$438,657, respectively, for PV/BS, PV/FC, and PV/FC/BS. The integration between BS and FC decreased the NPC by 34.28% and 13.21% compared to PV/BS and PV/FC, respectively. On the other hand, the values of COE are \$0.164/kWh, \$0.124/kWh, \$0.117/kWh, respectively, for PV/BS, PV/FC, and PV/FC/BS. Under this condition using PV/FC/BS reduces the cost of energy by 28.66% and 5.6% compared to PV/BS and PV/FC, respectively. In addition, the considered systems were compared with the grid extension to explore the best power system to meet the load demand. The results of the comparison confirmed that the PV/FC/BS system is better than the UG extension up to a distance of 16.1 km, while PV/BS is better than the grid extension up to a distance of 26.6 km.

Author Contributions: Conceptualization, H.A.Z. and H.R.; methodology, H.A.Z.; software, H.R.; validation, M.A. and H.A.Z.; formal analysis, H.R.; investigation, H.A.Z.; resources, H.R.; data curation, H.R.; writing—original draft preparation, M.A. and H.A.Z.; writing—review and editing, H.R.; visualization, H.A.Z.; supervision, H.R.; project administration, H.A.Z.; funding acquisition, M.A. All authors have read and agreed to the published version of the manuscript.

Funding: This research received no external funding.

Acknowledgments: The author (M.A.) would like to thank Shaqra University, Saudi Arabia to support him in this work.

Conflicts of Interest: The authors declare no conflict of interest.

References

1. Saudi Aramco's First-half 2019 Financial Reports, for the Six Months Ended June 30, 2019. Available online: <https://www.saudiaramco.com> (accessed on 14 February 2020).
2. Saudi Arabia's Vision 2030. Available online: <https://vision2030.gov.sa> (accessed on 17 February 2020).
3. DeNicola, E.; Aburizaiza, O.S.; Siddique, A.; Khwaja, H.; Carpenter, D.O. Review: Climate Change and Water Scarcity: The Case of Saudi Arabia. *Ann. Glob. Health* **2015**, *81*. [CrossRef]
4. Aly, H. Royal Dream: City Branding and Saudi Arabia's NEOM. *Middle East Topics Argum.* **2019**. [CrossRef]
5. Farag, A.A. The Story of NEOM City: Opportunities and Challenges. In *New Cities and Community Extensions in Egypt and the Middle East: Visions and Challenges*; Chapter in Book; Attia, S., Shafik, Z., Ibrahim, A., Eds.; Springer: Cham, Switzerland, 2019; ISBN 978-3-319-77874-7. [CrossRef]
6. Alkaisi, A.; Mossad, R.; Sharifian-Barforoush, A. A review of the water desalination systems integrated with renewable energy. *Energy Procedia* **2017**, *110*, 268–274. [CrossRef]
7. Gude, V.G. *Renewable Energy Powered Desalination Handbook: Application and Thermodynamics*; Butterworth-Heinemann: Oxford, UK, 2018; ISBN 978-0-12-815244-7. [CrossRef]
8. Hasan, E. Desalination Integration with Renewable Energy for Climate Change Abatement in the MENA Region. *Recent Prog. Desalin. Environ. Mar. Outfall Syst.* **2015**, *1*, 159–173. [CrossRef]
9. Xevgenos, D.; Moustakas, K.; Malamis, D.; Loizidou, M. An overview on desalination and sustainability: Renewable energy-driven desalination and brine management. *Desalin. Water Treat.* **2016**, *57*, 2304–2314. [CrossRef]
10. Ruiz-García, A.; Melián-Martel, N.; Nuez, I. Short Review on Predicting Fouling in RO Desalination. *Membranes* **2017**, *7*, 62. [CrossRef]
11. Melián-Martel, N.; Alonso, J.; Ruiz-García, A. Combined silica and sodium alginate fouling of spiral-wound reverse osmosis membranes for seawater desalination. *Desalination* **2018**, *439*, 25–30. [CrossRef]
12. Abdel-Salam, M.; Ahmed, A.; Ziedan, H.; Sayed, K.; Amery, M.; Swify, M. A Solar-wind Hybrid Power System for Irrigation Toshka Area. In Proceedings of the 2011 IEEE Jordan Conference on Applied Electrical Engineering and Computing Technologies (AEECT), Amman, Jordan, 6–8 December 2011. [CrossRef]
13. Rezk, H.; Abdelkareem, M.A.; Ghenai, C. Performance evaluation and optimal design of stand-alone solar PV-battery system for irrigation in isolated regions: A case study in Al Minya (Egypt). *Sustain. Energy Technol. Assess.* **2019**, *36*, 100556. [CrossRef]
14. Rezk, H.; Sayed, E.T.; Al-Dhaifallah, M.; Obaid, M.; El-Sayed, A.H.M.; Abdelkareem, M.A.; Olabi, A.G. Fuel cell as an effective energy storage in reverse osmosis desalination plant powered by photovoltaic system. *Energy* **2019**, *175*, 423–433. [CrossRef]
15. Mohamed, M.A.; Diab, A.A.Z.; Rezk, H. Partial shading mitigation of PV systems via different meta-heuristic techniques. *Renew. Energy* **2019**, *130*, 1159–1175. [CrossRef]
16. Abdalla, O.; Rezk, H.; Ahmed, E.M. Wind driven optimization algorithm based global MPPT for PV system under non-uniform solar irradiance. *Sol. Energy* **2019**, *180*, 429–444. [CrossRef]
17. Sarma, U.; Ganguly, S. Design optimisation for component sizing using multi-objective particle swarm optimisation and control of PEM fuel cell-battery hybrid energy system for locomotive application. *Iet Electr. Syst. Transp.* **2020**, *10*, 52–61. [CrossRef]
18. Vijay, A.; Hawkes, A. Impact of dynamic aspects on economics of fuel cell based micro co-generation in low carbon futures. *Energy* **2018**, *155*, 874–886. [CrossRef]
19. Abdelkareem, M.A.; Allagui, A.; Sayed, E.T.; El Haj, A.M.; Said, Z.; Elsaid, K. Comparative analysis of liquid versus vapor-feed passive direct methanol fuel cells. *Renew. Energy* **2019**, *131*, 563–584. [CrossRef]
20. Zhang, X.; Chan, S.H.; Ho, H.K.; Tan, S.C.; Li, M.; Li, G.; Li, J.; Feng, Z. Towards a smart energy network: The roles of fuel/electrolysis cells and technological perspectives. *Int. J. Hydrog. Energy* **2015**, *40*, 6866–6919. [CrossRef]
21. Ameri, M.; Yoosefi, M. Power and fresh water production by solar energy, fuel cell, and reverse osmosis desalination. *J. Renew. Energy Environ.* **2016**, *3*, 25–34.

22. Rehman, S.; Habib, H.U.R.; Wang, S.; Büker, M.S.; Alhems, L.M.; Al Garni, H.Z. Optimal Design and Model Predictive Control of Standalone HRES: A Real Case Study for Residential Demand Side Management. *IEEE Access* **2020**. [[CrossRef](#)]
23. Al-Ammar, E.A.; Habib, H.U.R.; Kotb, K.M.; Wang, S.; Ko, W.; Elmorshedy, M.F.; Waqar, A. Residential Community Load Management Based on Optimal Design of Standalone HRES With Model Predictive Control. *IEEE Access* **2020**, *8*. [[CrossRef](#)]
24. Shafik, M.B.; Rashed, G.I.; Chen, H. Optimizing Energy Savings and Operation of Active Distribution Networks Utilizing Hybrid Energy Resources and Soft Open points: Case Study in Sohag, Egypt. *IEEE Access* **2020**. [[CrossRef](#)]
25. Ziedan, H.A.; Elbaset, A.A.; Mourad, A.N. Optimization of PV/Wind Power System: Case study: Supplying Large Industry Load in Egypt. *J. Eng. Appl. Sci.* **2020**, *15*, 1014–1020. [[CrossRef](#)]
26. Al-Ghussain, L.; Samu, R.; Taylan, O.; Fahrioglu, M. Sizing Renewable Energy Systems with Energy Storage Systems in Microgrids for Maximum Cost-Efficient Utilization of Renewable Energy Resources. *Sustain. Cities Soc.* **2020**, 102059. [[CrossRef](#)]
27. Habib, H.U.R.; Wang, S.; Elkadeem, M.R.; Elmorshedy, M.F. Design Optimization and Model Predictive Control of a Standalone Hybrid Renewable Energy System: A Case Study on a Small Residential Load in Pakistan. *IEEE Access* **2019**, *7*. [[CrossRef](#)]
28. Fodhil, F.; Hamidat, A.; Nadjemi, O. Potential, optimization and sensitivity analysis of photovoltaic-diesel-battery hybrid energy system for rural electrification in Algeria. *Energy* **2019**, *169*, 613–624. [[CrossRef](#)]
29. Jahangiri, M.; Haghani, A.; Shamsabadi, A.; Mostafaeipour, A.; Pomares, L.M. Feasibility study on the provision of electricity and hydrogen for domestic purposes in the south of Iran using grid-connected renewable energy plants. *Energy Strategy Rev.* **2019**, *23*, 23–32. [[CrossRef](#)]
30. Aziz, A.S.; Tajuddin, M.F.N.; Adzman, M.R.; Azmi, A.; Ramli, M.A. Optimization and sensitivity analysis of standalone hybrid energy systems for rural electrification: A case study of Iraq. *Renew. Energy* **2019**, *138*, 775–792. [[CrossRef](#)]
31. Aziz, A.S.; Tajuddin, M.F.N.; Adzman, M.R.; Ramli, M.A.; Mekhilef, S. Energy management and optimization of a PV/diesel/battery hybrid energy system using a combined dispatch strategy. *Sustainability* **2019**, *11*, 683. [[CrossRef](#)]
32. Acevedo-Arenas, C.Y.; Correcher, A.; Sánchez-Díaz, C.; Ariza, E.; Alfonso-Solar, D.; Vargas-Salgado, C.; Petit-Suárez, J.F. MPC for optimal dispatch of an AC-linked hybrid PV/wind/biomass/H₂ system incorporating demand response. *Energy Convers. Manag.* **2019**, *186*, 241–257. [[CrossRef](#)]
33. Awan, A.B. Performance analysis and optimization of a hybrid renewable energy system for sustainable NEOM city in Saudi Arabia. *J. Renew. Sustain. Energy* **2019**, *11*. [[CrossRef](#)]
34. Akar, O.; Terzi, Ü.K.; Tunçalp, B.K.; Sönmezocak, T. Determination of the Optimum Hybrid Renewable Power System: A case study of Istanbul Gedik University Gedik Vocational School. *Balk. J. Electr. Comput. Eng.* **2019**, *7*. [[CrossRef](#)]
35. Oladigbolu, J.O.; Ramli, M.A.; Al-Turki, Y.A. Techno-Economic and Sensitivity Analyses for an Optimal Hybrid Power System Which is Adaptable and Effective for Rural Electrification: A Case Study of Nigeria. *Sustainability* **2019**, *11*, 4959. [[CrossRef](#)]
36. Goudarzi, S.A.; Fazelpour, F.; Gharehpetian, G.B.; Rosen, M.A. Techno-economic assessment of hybrid renewable resources for a residential building in Tehran. *Environ. Prog. Sustain. Energy* **2019**, *38*, 13209. [[CrossRef](#)]
37. Shaahid, S.M.; Alhems, L.M.; Rahman, M.K. Techno-economic assessment of establishment of wind farms in different Provinces of Saudi Arabia to mitigate future energy challenges. *Therm. Sci.* **2019**, *23*, 2909–2918. [[CrossRef](#)]
38. Alyahya, S.; Irfan, M. Analysis from the New Solar Radiation Atlas for Saudi Arabia. *Sol. Energy* **2016**, *130*, 116–127. [[CrossRef](#)]
39. NASA. Surface Meteorology and Energy. Available online: <https://power.larc.nasa.gov> (accessed on 17 February 2020).
40. Rezk, H.; Dousoky, G.M. Technical and economic analysis of different configurations of stand-alone hybrid renewable power systems—A case study. *Renew. Sustain. Energy Rev.* **2017**, *62*, 941–953. [[CrossRef](#)]

41. Rezk, H.; Shoyama, M. Techno-economic optimum sizing of stand-alone photovoltaic/fuel cell renewable system for irrigation water pumping applications. In Proceedings of the IEEE International Conference on Power and Energy (PECon), Kuching, Sarawak, Malaysia, 1–3 December 2014; pp. 182–186.
42. Said, M.M.; El-Aassar, A.M.; Kotp, Y.H.; Shawky, H.A.; Abdel Mottaleb, M.S. Performance assessment of prepared polyamide thin film composite membrane for desalination of saline groundwater at Mersa Alam-Ras Banas, Red Sea Coast, Egypt. *Desalin. Water Treat.* **2013**. [[CrossRef](#)]
43. Singh, O.; Turkiya, S. A survey of household domestic water consumption patterns in rural semi-arid village, India. *GeoJournal* **2013**, *78*, 777–790. [[CrossRef](#)]
44. MAK Water. Available online: <https://www.makwater.com.au/products/sea-water-reverse-osmosis/> (accessed on 17 February 2020).
45. Ruiz-García, A.; Nuez, I. Long-term performance decline in a brackish water reverse osmosis desalination plant. Predictive model for the water permeability coefficient. *Desalination* **2016**, *397*, 101–107. [[CrossRef](#)]
46. Kim, J.; Park, K.; Yang, D.R.; Honga, S. A comprehensive review of energy consumption of seawater reverse osmosis desalination plants. *Appl. Energy* **2019**, *254*, 113652. [[CrossRef](#)]
47. Ruiz-García, A.; Feo-García, J. Operating and maintenance cost in seawater reverse osmosis desalination plants. Artificial neural network based model. *Desalin. Water Treat.* **2017**, *73*, 73–79. [[CrossRef](#)]
48. Abo-Elyousr, F.K.; Nozhy, A.N. Bi-objective Economic Feasibility of Hybrid Micro-Grid Systems with Multiple Fuel Options for Islanded Areas in Egypt. *Renew. Energy* **2018**. [[CrossRef](#)]
49. Rosewater, D.M.; Copp, D.A.; Nguyen, T.A.; Byrne, R.H.; Santoso, S. Battery Energy Storage Models for Optimal Control. *IEEE Access* **2019**, *7*, 178357–178391. [[CrossRef](#)]
50. Dursun, B.; Aykut, E. An investigation on wind/PV/fuel cell/battery hybrid renewable energy system for nursing home in Istanbul. *J. Power Energy Part A* **2019**. [[CrossRef](#)]
51. Li, C. Techno-economic study of off-grid hybrid photovoltaic/battery and photovoltaic/battery/fuel cell power systems in Kunming, China. *Energy Sources Part A Recovery Util. Environ. Eff.* **2018**. [[CrossRef](#)]
52. Sayed, K.; Gronfula, M.G.; Ziedan, H.A. Novel Soft-Switching Integrated Boost DC-DC Converter for PV Power System. *Energies* **2020**, *13*, 749. [[CrossRef](#)]
53. Nejati, S.; Mirbagheri, S.A.; Warsinger, D.M.; Fazeli, M. Biofouling in seawater reverse osmosis (SWRO): Impact of module geometry and mitigation with ultrafiltration. *J. Water Process Eng.* **2019**, *29*, 100782. [[CrossRef](#)]
54. Feo-García, J.; Ruiz-García, A.; Ruiz-Saavedra, E.; Melian-Martel, N. Energy consumption assessment of 4000 m³/d SWRO desalination plants. *Desalin. Water Treat.* **2016**, *57*, 23019–23023. [[CrossRef](#)]
55. Saudi Electricity Company. Available online: <https://www.se.com.sa> (accessed on 14 February 2020).



© 2020 by the authors. Licensee MDPI, Basel, Switzerland. This article is an open access article distributed under the terms and conditions of the Creative Commons Attribution (CC BY) license (<http://creativecommons.org/licenses/by/4.0/>).